Quantitative estimation of brain tumor angiogenesis *in vivo*

N. S. Akella[1], D. B. Twieg[1], L. B. Nabors[2]

[1]Biomedical Engineering, University of Alabama at Birmingham, Birmingham, AL, United States, [2]Neurology, University of Alabama at Birmingham, Birmingham, AL, United States

OVERVIEW

Ever since research has shown that tumor growth is angiogenesis dependent[1], the understanding and monitoring of tumor angioarchitecture has become central to tumor therapy and management. The T_2* susceptibility physics of paramagnetic contrast agents can be utilized to measure blood kinetics *in vivo* with a temporal resolution of 1-2 seconds, using fast echo-planar MR imaging techniques. Traditionally, parametric maps of hemodynamic parameters like relative cerebral blood volume (CBV), relative cerebral blood flow (CBF) and mean transit time (MTT) have been used to report tumor characteristics, often aiding diagnoses. Parametric maps do however have a drawback in that they do not fully present the spatiotemporal information of the cerebral hemodynamics. Perfusion data sets also contain hemodynamic information like MR signal drop, bolus arrival time, T_2* recovery etc. We propose and test a model to quantitatively estimate angiogenesis based on empirical changes to perfusion parameters. This work is one of the first attempts to quantify angiogenesis on a pixel-by-pixel basis.

THEORY AND METHODS

MR Imaging Dynamic susceptibility-enhanced contrast (DSC) perfusion MR imaging sequences were run on a 1.5 T scanner (Signa 5.7, GE Medical Systems, Milwaukee, WI). Five patients with clinically diagnosed high-grade (WHO grade III and IV) unifocal malignant gliomas were imaged using the gradient recalled echo-planar imaging sequence (TR/TE = 1900/65 ms, FOV = 24 cm^2, 6mm slices). 65 images were acquired for the perfusion series, resulting in a total imaging time of around 2 minutes. The contrast agent (Magnevist, 0.2 mmol/kg of patient body weight) was injected with a power injector at a flow rate of 4.0 ml/sec and an injection delay of 15 seconds. Spin-echo post-contrast T_1 weighted images (TR/TE of 450/10 ms) were acquired following perfusion imaging for anatomic reference. All imaging studies were approved by our hospital committees.

Image Analysis and Post-processing Post processing and perfusion analysis were performed using the MedX software (Medical Numerics Inc., Sterling, VA) running on a Sun Blade 1000 workstation (Sun Microsystems, Palo Alto, CA). The data sets were prepared for post-processing by inspection for quality, masking, and generation of parametric maps. A two-stage automated algorithm[2] was used for identifying arterial voxels in the perfusion MRI data and constructing the arterial input function (AIF). The relative CBV maps were determined though gamma-variate fitting[3] of the concentration curves and integration. The relative CBF maps were generated from the amplitude of the residue curve which results from deconvolution of the tissue curve via singular value decomposition. The T_2* recovery of every pixel was computed by calculating the mean signal intensity of the last 20 perfusion-series images as a percentage of the pre-contrast maximum. All subsequent image analyses were then performed using custom written programs in MATLAB (The MathWorks Inc., Natick, MA).

Angiogenesis Computation We model angiogenesis as $\boldsymbol{A} = k \cdot V \cdot F / T_{2\,rec}^{*}$, where $\boldsymbol{A}$ is the Angiogenesis potential, V is the relative CBV, F is the relative CBF and $T_{2\,rec}^{*}$ is the T_2* recovery computed from the signal-time curve of the perfusion study, and k is an arbitrary constant. $\boldsymbol{A}$ is computed pixel-by-pixel and the maps are overlaid onto the post-contrast T_1 weighted images. The next step was to investigate the spatial variance of angiogenesis in regions of brain affected by the tumor. The tumor enhancing area was outlined and the centroid (planar center of mass) of the tumor was computed. Pixels were classified into concentric annular regions of increasing radii based on their Euclidean distance from the tumor centroid, illustrated in figure 1. Mean $\boldsymbol{A}$, V, F and $T_{2\,rec}^{*}$ were computed for these regions and plotted as a function of the radius. A reference ROI was placed in the uninvolved hemisphere of the brain and similar calculations were performed for comparison with normal tissue.

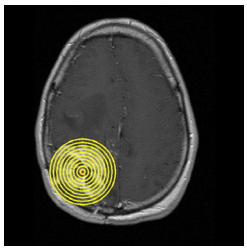

Figure 1 Angiogenesis computation model: The red asterisk represents the tumor centroid while regions between the yellow circles represent the annular ROIs.

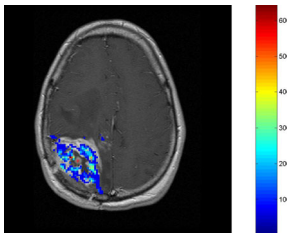

a

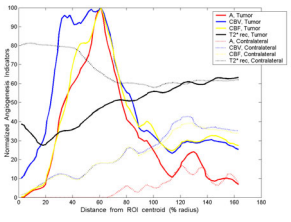

b

Figure 2 (a) The $\boldsymbol{A}$ map overlaid on a post-contrast T1 weighted image, and (b) normalized plots of $\boldsymbol{A}$ and other indices as functions of distance from tumor centroid, computed using our model.

RESULTS AND DISCUSSION

The $\boldsymbol{A}$ maps generated using our model are shown in Figure 2(a). The spatial variance of the empirically determined angiogenesis potential is shown in figure 2(b), where values of $\boldsymbol{A}$ and other indices are plotted as a function of the distance from the centroid of the tumor. All 5 subjects exhibited similar spatial variance of $\boldsymbol{A}$, with the maximum value between 50-80% of tumor radius from the centroid. This suggests that angiogenesis is predominant in the fringe areas of the tumor. The central regions typically have low angiogenesis depending on the extent of necrosis in the subjects. Our results are consistent with histology reports of microvasculature in high grade malignant gliomas published earlier. The parameter $\boldsymbol{A}$ is flexible; it is possible to vary the weights of flow, volume and other parameters to suit the specific tumor biology being studied. The model is also easily extended to three spatial dimensions. Quantitative approaches such as ours will help with treatment planning, therapy monitoring and prognostic assessment of tumor growth *in vivo*.

REFERENCES

[1] Folkman. J. J Natl Cancer Inst 1990; 82:4-6.
[2] Morris ED, et al. TA. Proc. ISMRM. 2000; 8:740.
[3] Ostergaard L, et al.. Magn Reson Med 1996; 36:715-725.

ACKNOWLEDGEMENTS

This work was supported by NIH grant R21 CA 091560